7-2013

Characterizing Acoustic Fluidized Bed Hydrodynamics Using X-Ray Computed Tomography

David R. Escudero
Iowa State University, drescude@iastate.edu

Theodore J. Heindel
Iowa State University, theindel@iastate.edu

Characterizing Acoustic Fluidized Bed Hydrodynamics Using X-Ray Computed Tomography

Abstract
Fluidized bed reactors are important assets of many industrial applications because they provide uniform temperature distributions, low pressure drops, and high heat/mass rates. Characterizing the hydrodynamics of a fluidized bed is important to better understand the behavior of these multiphase flow systems. The hydrodynamic behavior in a cold flow 3D fluidized bed, with and without acoustic intervention, using X-ray computed tomography is investigated in this study. Experiments are carried out in a 10.2 cm ID fluidized bed filled with glass beads, with material density of 2600 kg/m^3 and particle size ranges between 212–600 μm. In this study, three different bed height-to-diameter ratios are examined: H/D = 0.5, 1 and 1.5. Moreover, the sound frequency of the loudspeaker used as the acoustic source is fixed at 150 Hz with a sound pressure level of 120 dB. Local time-average gas holdup results show that the fluidized bed under the presence of an acoustic field provides a more uniform fluidization, the bed exhibits less channeling, and the jetting phenomena produced by the distributor plate is less prominent when compared to no acoustic field. Thus, acoustic intervention affects the hydrodynamic behavior of the fluidized bed.

Keywords
Acoustic fluidized bed, hydrodynamics, x-ray computed tomography

Comments
This is a conference proceeding from *ASME 2013 Fluids Engineering Division Summer Meeting* 2 (2013): 1, doi:10.1115/FEDSM2013-16094. Posted with permission.

Proceedings of the ASME 2013 Fluids Engineering Division Summer Meeting
FEDSM2013
July 7-11, 2013, Incline Village, Nevada, USA

FEDSM2013-16094

CHARACTERIZING ACOUSTIC FLUIDIZED BED HYDRODYNAMICS USING X-RAY COMPUTED TOMOGRAPHY

David R. Escudero[†] and Theodore J. Heindel
Department of Mechanical Engineering
Iowa State University
Ames, Iowa 50011

ABSTRACT

Fluidized bed reactors are important assets of many industrial applications because they provide uniform temperature distributions, low pressure drops, and high heat/mass rates. Characterizing the hydrodynamics of a fluidized bed is important to better understand the behavior of these multiphase flow systems. The hydrodynamic behavior in a cold flow 3D fluidized bed, with and without acoustic intervention, using X-ray computed tomography is investigated in this study. Experiments are carried out in a 10.2 cm ID fluidized bed filled with glass beads, with material density of 2600 kg/m^3 and particle size ranges between 212-600 μm. In this study, three different bed height-to-diameter ratios are examined: H/D = 0.5, 1 and 1.5. Moreover, the sound frequency of the loudspeaker used as the acoustic source is fixed at 150 Hz with a sound pressure level of 120 dB. Local time-average gas holdup results show that the fluidized bed under the presence of an acoustic field provides a more uniform fluidization, the bed exhibits less channeling, and the jetting phenomena produced by the distributor plate is less prominent when compared to no acoustic field. Thus, acoustic intervention affects the hydrodynamic behavior of the fluidized bed.

Keywords: Acoustic fluidized bed, hydrodynamics, X-ray computed tomography.

INTRODUCTION

Acoustic fluidized beds have been studied for different Geldart type particles (Geldart type A-C) to understand the effects produced by the acoustic field on the fluidization behavior and quality. This is an attractive option because it is a non-invasive technique that does not change the internal structure of the bed and there is no limitation to the particle type that can be fluidized.

Leu et al. [1] studied the fluidization of Geldart type B particles in an acoustic fluidized bed. They determined the influence of the speaker power, sound frequency, particle loading, and distance between the speaker and bed surface on the hydrodynamic properties of a fluidized bed filled with 194 μm sand. They found that when an acoustic field is applied, a different particle loading height creates a different minimum fluidization velocity, making minimum fluidization velocity dependent on bed height. They also showed that the standard deviation of the pressure fluctuations and the bubble rise velocity were reduced in the presence of an acoustic field.

Guo et al. [2] investigated the behavior of ultrafine (Geldart type C) particles under the influence of sound waves. They studied both nanometer and micrometer size particles. They found that as frequency increased, the minimum fluidization velocity decreased and then after a specified frequency (40-50 Hz), the minimum fluidization velocity increased. When the sound pressure level was changed (100 dB - 103.4 dB) and the sound frequency remained fixed, the minimum fluidization velocity decreased for all particles, thus improving the fluidization quality of the particles. The same trends were found by Kaliyaperumal et al. [3] and Levy et al. [4].

Herrera and Levy [5] used visual observations as well as invasive techniques such as fiber optic probes to measure the bubbling characteristic of a Geldart type A fluidized bed. Using these techniques they determined that high values of the sound pressure level affected the fluidization behavior of the bed, and

[†]Corresponding Author: David Escudero (drescude@iastate.edu)

had a large impact on the bubble characteristics, such as size and frequency.

Moreover, Guo et al. [6] analyzed the effects of the acoustic field on a fluidized bed at different temperatures for quartz sand (74 μm, 2650 kg/m^3) and SiO_2 particles (0.5 μm, 2560 kg/m^3) using pressure transducer and pressure fluctuations analysis as a measurement technique. The results obtained in that study showed that minimum fluidization velocity decreased with increasing temperature with, as well as without, acoustic assistance. In the same way, at a fixed sound pressure level (120 dB), the minimum fluidization velocity decreased when the frequency was increased from 50-200 Hz, and then the minimum fluidization velocity increased with frequency from 200-400 Hz.

Si and Guo [7] studied how an acoustic fluidized bed improved the fluidization of two different biomass particles, sawdust and wheat stalks, alone or mixed with quartz sand. They compared the fluidization behavior of the biomass without and with the acoustic field to determine if there was any improvement due to the acoustic field. Additionally, they determined the effects that the sound pressure level (SPL) had on the minimum fluidization velocity. Initially, they found that the biomass by itself fluidized poorly with and without the presence of the acoustic field. Then, they added quartz sand to aid fluidization and maintained the biomass mass fraction at 60%. They observed that below a SPL of 90 dB, plugging and channeling occurred in the fluidized bed. Increasing the SPL diminished the effects of channeling and improved the quality of fluidization. By varying the sound frequency between 50 to 400 Hz, they determined that the minimum fluidization velocity decreased with increasing frequency until it reached a minimum value and then increased with increasing frequency.

Si and Guo [7] also fixed the sound frequency at 150 Hz and varied the sound pressure level between 90 and 120 dB. Using these conditions, they determined the effects on the minimum fluidization velocity. They found that, when the sound pressure level was above 100 dB, the fluidization quality improved, and they observed that the biomass mixture fluidized smoothly without any obvious slugging or channeling. All of their conclusions were obtained using visual observations.

X-rays have been used to study gas-solid fluidized beds as well as two and three phase fluidized systems for more than 50 years [8]. They are a commonly employed noninvasive technique because they are safer than other nuclear based techniques which cannot be turned on and off at will, have high resolution, and can be controlled by varying the voltage or current to improve penetration or contrast [9].

X-ray computed tomography (XCT) can generate a 3D image of the object of interest. X-rays pass through the object and the intensity values are recorded from several projections by an imaging device. After the images are collected, computer algorithms reconstruct the images to produce a 3D representation of the object. However, due to the number of projections that must be acquired in order to obtain a whole reconstruction of the object, this technique does not have a good temporal resolution. On the other hand, having multiple scans from different projections give a high spatial resolution to this technique, a characteristic that can be used to measure the local time-average gas holdup in a very efficient way. [10]

Moreover, XCT data analysis allows for the calculation of time-average local gas holdup or solid holdup. Grassler and Wirth [11] used XCT to determine the solids concentration in a 0.19 m diameter circulating fluidized bed with 50-70 μm glass beads as the bed material. Tests were carried out in two different systems. In the first, solid concentrations were calculated with an up flow system. Results for this system showed that radial solid concentration exhibited a parabolic shape with a maximum concentration close to the wall of the reactor and a minimum concentration in the center of the bed. For the second, the solid concentration was calculated with a down flow system. For this case, the solid concentration distribution was much more complex and depended upon the gas-solids distributor operating conditions. Results showed various solid concentration distributions from a homogeneous distribution with a parabolic profile to concentrated strands in the center of the bed. Finally, the study also showed that the solids concentration was accurately calculated within 5% error for concentrations up to 20 vol% with a minimum resolution of 0.2 mm.

Escudero and Heindel [10, 12] studied the effects of bed height, superficial gas velocity, and bed material on the local time-average gas holdup of a 10.2 cm fluidized bed, using X-ray computed tomography. Using different materials (glass beads, ground corncob, and ground walnut shell), superficial gas velocities (U_g), and height-to-diameter ratio (H/D), they determined the variations on the fluidization hydrodynamics of the bed. They found that as superficial gas velocity increased, the overall gas holdup increased for every bed height studied. Flow behavior was also affected with the increase in superficial gas velocity. Increasing bed height, particularly at the higher gas flow rates, enhanced bubble coalescence creating slugs that flow thorough the center of the bed, producing regions of low gas holdup near the walls of the fluidized bed. Also, the effects of bed height observed in the time-average local gas holdup vary depending of the bed material tested.

Finally, as material density decreases, gas holdup increases. Glass beads have lower gas holdup than both ground walnut shell and ground corncob, while ground corncob exhibited the largest gas holdup of all three materials in this study. Ground corncob also exhibited a better distribution of gas holdup along the entire bed, therefore providing a more uniform fluidization.

Most of the studies on acoustic fluidized beds available in the literature used both invasive and noninvasive measurement techniques to obtain the hydrodynamic characteristics of the bed. Fiber optic systems, visual observations, pressure analysis or camcorder systems are examples of some of the techniques used in some of the studies summarized in the previous paragraphs. However, non-invasive techniques such as X-ray computed tomography have not been used in sound assisted fluidized bed to determine qualitative and quantitative hydrodynamic characteristics. The goal of this study is to

alleviate this shortcoming and characterize the hydrodynamics of an acoustic 3D fluidized bed using X-ray computed tomography.

EXPERIMENTAL SETUP

The reactor used in these experiments is a cold flow fluidized bed reactor. The cylindrical fluidized bed was fabricated with D = 10.2 cm internal diameter (ID) acrylic with a 0.64 cm wall thickness. As shown in Figure 1, the reactor consists of three main chambers: the top chamber or freeboard region, the bed chamber, and the plenum. Fluidization occurs in the bed chamber which is 30.5 cm tall and 10.2 cm ID. Square flanges (16.5×16.5 cm) connect each section. An aeration plate is located immediately below the bed chamber; it is fabricated from a 1.27 cm thick acrylic plate with 62, 1 mm diameter holes spaced approximately 1.27 cm apart on a circular grid for a total open area of 0.62%.

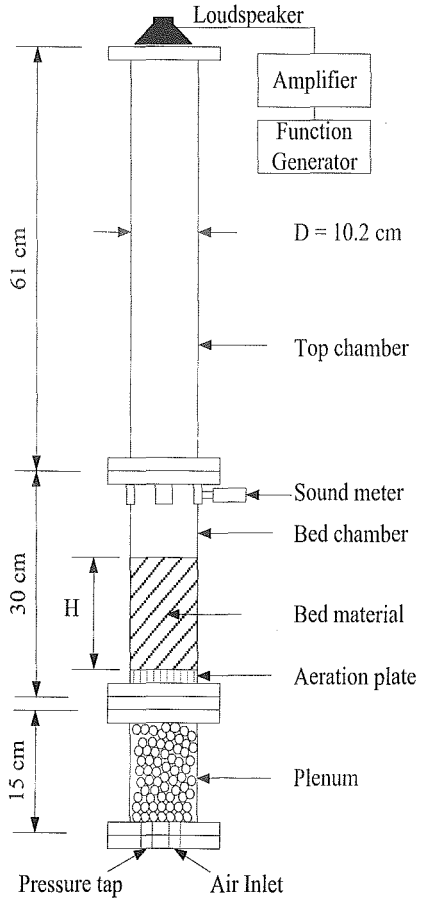

FIGURE 1: FLUIDIZED BED REACTOR (NOT TO SCALE). THE STATIC BED HEIGHT IS IDENTIFIED BY H.

Compressed air from the laboratory's building air supply is used as the fluidizing gas for this research. The pressure at which the compressed air is delivered inside the laboratory is 620 kPa (90 psi). However, since the flow rates used for fluidization vary depending of the specific conditions of each experiment, an air flow control board with four independent air lines is used to deliver the required air to the fluidized bed.

The fluidized bed air flow is regulated using a stepper motor valve Aalborg SMV40-SVF2-A. The regulated air flows through a 0-1000 Lpm stainless steel Aalborg GFM771 flow meter.

The fluidizing material used in this study is glass beads (ρ_{glass} = 2600 kg/m^3) over three different size ranges (212-425 μm, 425-500 μm, and 500-600 μm). The bed bulk density is determined knowing the material mass and the static bed volume. Bed material is slowly added until the desired static bed height is reached, which corresponds to H/D = 0.5, 1, and 1.5. Before the bed height is measured, the bed is fluidized and then allowed to collapse to avoid any packing effects due to the filling process. The material mass is then measured and the given bed bulk density is calculated. Table 1 summarizes the general bed characteristics.

TABLE 1: SUMMARY OF BED CHARACTERISTICS.

Glass Beads			
H/D	**0.5**	**1**	**1.5**
Bed Mass (g)	625	1250	1845
Bulk density (kg/m^3)	1515	1515	1495
Diameter (μm)	212-425, 425-500, 500-600		
Particle Density (kg/m^3)	2600		

To avoid electrostatic effects that may build up during fluidization, the fluidization air is passed through a humidifier before entering the fluidized bed inlet. Several trials in the laboratory have shown that using this simple solution minimized electrostatic effects.

X-ray computed tomography (CT) scans are captured with and without acoustic intervention at different H/D ratios (0.5, 1, 1.5) and different superficial gas velocities U_g = 1.5 and 3 U_{mf}, where U_{mf} is the minimum fluidization velocity previously determined [13].

The X-ray equipment used in this research is described in detail by Heindel et al. [14], and only the procedure used for this study is described here. First, the X-ray source that is located opposite the CT detector is warmed up at the same time the thermoelectric cooler on the camera is simultaneously cooled to 0°C to reduce noise and allow for long CT scans. Custom X-ray imaging software captures the CT images, controls the camera settings, and controls the rotation ring motion. After completing the warm-up process, the X-ray voltage and current, as well as the camera exposure time and binning options are adjusted. For this study, the power settings are constant at a voltage of 150 keV and a current of 3 mA, and the exposure time is set to 1 second and the binning is set to 4×4. Next, the fluidized bed is placed in the imaging region and the scintillation crystals in the detector are excited with X-rays for about 20 minutes.

After the CT's are generated the files are transferred to a cluster at CNDE (Center for Nondestructive Evaluation) for reconstruction using standard algorithms [9]. Volume files are reconstructed and analyzed using custom software that allows

selecting the region of interest (ROI) in the image and generating 2-D images of different planes. For this study, three viewing axes are selected (Figure 2), images in the x-y plane at different heights, x-z plane in the center of the bed, and y-x plane passing through the center of the bed. A false color scale is then applied to each image to provide a better appreciation for the flow structure.

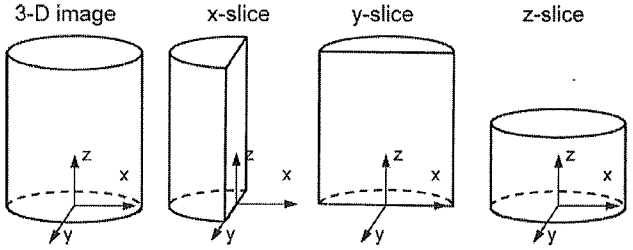

FIGURE 2: CT IMAGING SLICES PLANES [9].

Time-average local gas holdup information is calculated using the data obtained from the CT reconstruction volume files. Gas holdup is the amount of gas present in the solid material, and is useful to characterize the hydrodynamic behavior of the multiphase flow system. Quantifying the local time-average gas holdup, ε_g, requires the CT intensity of the empty reactor (I_g), a CT intensity of the reactor filled with a fixed bed of the bulk material (I_b), and a CT intensity of the reactor under specified fluidization conditions (I_f). To ensure the same response for each condition from the detector system, each CT is taken with the same X-ray source power settings for the respective conditions. The local time-average gas holdup is then determined from the two reference CT images and the flow CT image [10]:

$$\varepsilon_g = \frac{I_f - I_b + \left(I_g - I_f\right)\left(\varepsilon_{g,b}\right)}{I_g - I_b}$$

where the bulk void fraction, $\varepsilon_{g,b}$, is defined as:

$$\varepsilon_{g,b} = 1 - \frac{\rho_b}{\rho_p}$$

where ρ_b and ρ_p are the measured bulk and particle density, respectively. Further details of the data processing techniques are found in [10].

RESULTS AND DISCUSSION

Qualitative observations of the effects of acoustics on the time-average local gas holdup

Two-dimensional time-average local gas holdup maps sliced vertically through the fluidized bed centerline or horizontally at specified bed heights can be obtained to show qualitative characteristics of the bed material. Images of x-, y-, and z-slice gas holdup for 500-600 μm glass beads at a superficial gas velocity of $U_g = 3U_{mf}$ for different H/D ratios with and without the influence of an acoustic field are shown in Figure 3. The x- and y- slice images are taken through the center of the bed, while the z-slice images are taken at four different axial heights, h, measured from the aeration plate.

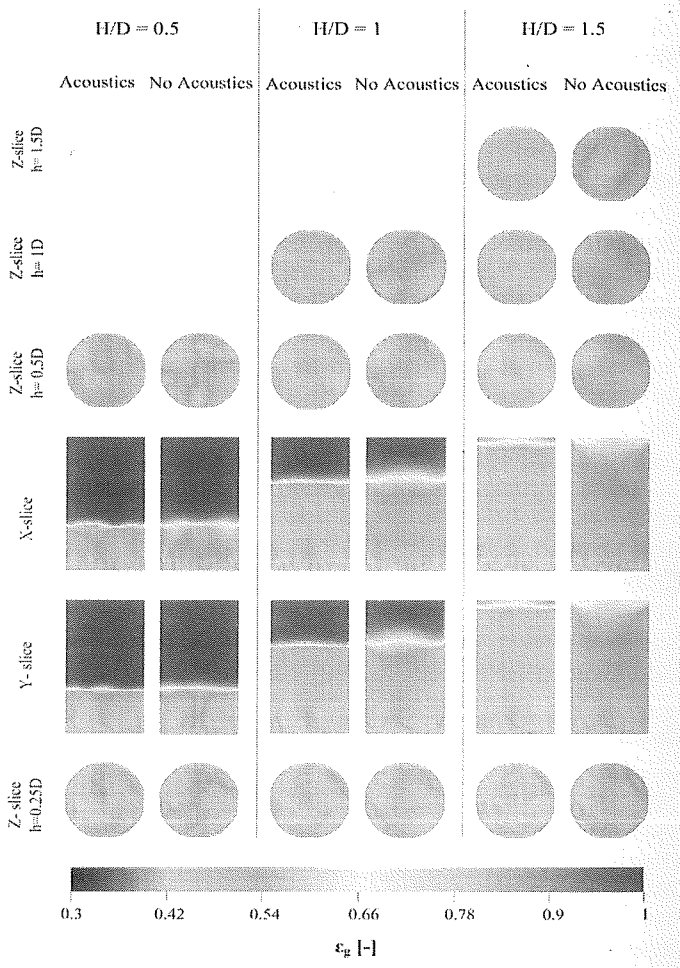

FIGURE 3: GAS HOLDUP FOR 500-600 μm GLASS BEADS AT DIFFERENT H/D RATIOS AND $U_g = 3U_{mf}$.

As shown in Figure 3, x- and y- slice images at every H/D ratio shows multiple air jets that are caused by the aeration holes of the distributor plate. More jetting can be observed in the images without the presence of an acoustic field, this phenomenon is attributed to the fact that the volume of air that is passing through the bed material is slightly higher than the flow rate that is passing through the bed with acoustic field presence because the minimum fluidization velocities are slightly different [13].

Moreover, the z-slice images located at h = 0.25D show that for the acoustic condition, some of the jets still have not merged with adjacent jets, which indicates zones of high gas holdup concentrations next to zones of low gas holdup concentration. In contrast, for the no acoustic condition, jet

merging has already happened at h = 0.25D, and the merged jet penetrate farther into the bed.

Similar hydrodynamic structures are observed in all the slices in Figure 3 for H/D = 0.5, independent of the presence of an acoustic field. However, as the H/D ratio increases, particularly when H/D > 0.5 and the bed height is far enough away from the aeration region, the hydrodynamic structures in the bed for both conditions differ. Gas holdup images from the acoustic bed show more uniform gas holdup concentration throughout the bed. This hydrodynamic structure may suggest that the acoustic vibration imposed to the system allows for more bed uniformity. On the other hand, the no acoustic images show higher gas holdup concentrations through the center of the bed and lower gas holdup concentration near the wall of the bed, suggesting that air is migrating toward the center of the bed, and it reaches the top of the bed, solid material is being thrown towards the wall, which falls back into the bed.

Furthermore, different glass bead particle sizes were tested in order to observe if acoustic effects are influenced by particle geometry. Figure 4 shows different 2D gas holdup maps for the three particles sizes tested at a H/D = 1 and a superficial gas velocity $U_g = 1.5U_{mf}$.

Similar hydrodynamic structures can be observed for the smallest glass bead particle size ranges (212-425, 422-500 μm) for both conditions, suggesting that the acoustic field does not produce a significant improvement in these ranges.

For the largest particle size range tested (500-600 μm), acoustics do have an effect on the structure of the bed. Looking at the z-slice located at h = 0.25D, acoustic condition has a lower gas holdup region near the walls of the bed, and a high gas holdup region in the center of the bed, meanwhile the no acoustic bed presents zones of high gas holdup region in the center and also near the walls of the bed. In the x-y-slices and in the z-slice located at h = 1D low gas holdup regions are located towards the wall of the acoustic fluidized bed, while the region in the center of the bed presents a high but uniform gas holdup region compared to the no acoustic fluidized bed.

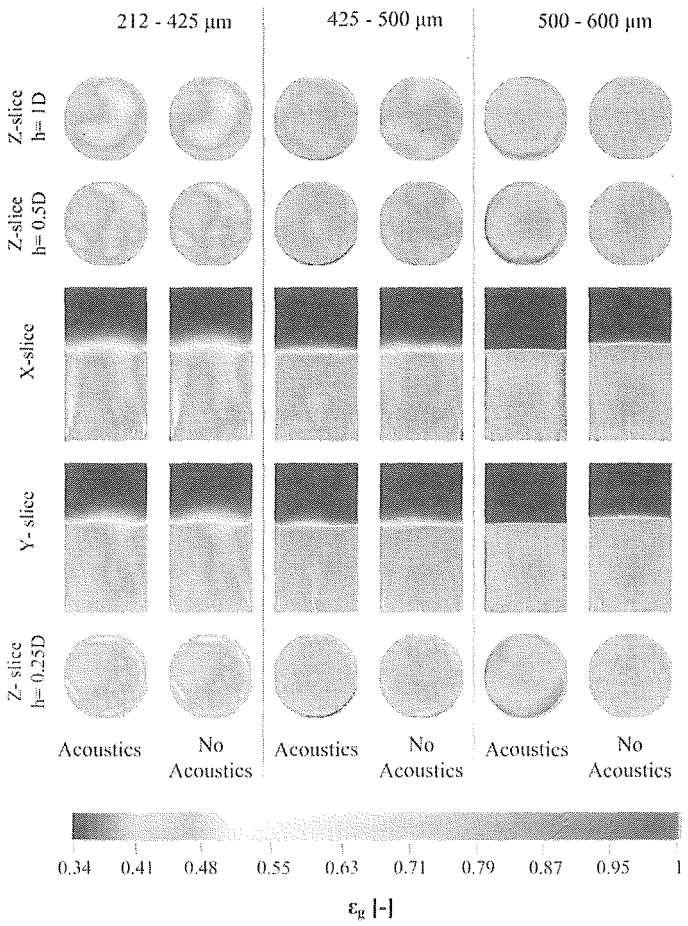

FIGURE 4: GAS HOLDUP AT $U_g = 1.5U_{mf}$ AND H/D = 1 FOR GLASS BEADS OF DIFFERENT PARTICLE SIZE RANGES.

Quantitative results of the effects of acoustics on the time-average local gas holdup

The horizontal averaged local time-average gas holdup is plotted as a function of height to determine quantitatively the variation of the gas holdup through the entire bed, with and without acoustic intervention. Figure 5 shows these trends for 500-600 μm glass beads at H/D = 1 for a superficial gas velocity of $U_g = 3U_{mf}$. As shown in Figure 5, at a lower bed height (h/D ≤ 0.25, where h is the local bed height measured from the aeration plate), both conditions presented variations that are attributed to the jetting phenomena near the distributor plate. As h/D increases (moving higher in the bed), gas holdup remains fairly constant for both cases; however, the acoustic condition shows a more uniform gas holdup distribution throughout the entire bed, which was also observed in the qualitative images (Figure 3 and 4). Near the top of the bed (h/D ≈ 1), the no acoustic condition has a higher bed expansion due to a slightly higher gas flow rate [13], which causes more material to be expelled from the bed. Similar trends as the ones shown in Figure 5 are observed when the superficial gas velocity changes.

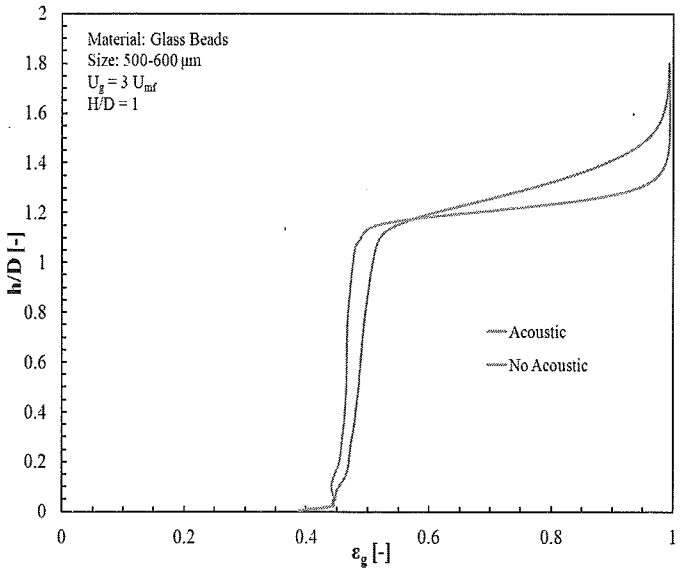

FIGURE 5: HORIZONTAL AVERAGE GAS HOLDUP FOR 500-600 µm GLASS BEADS WITH AND WITHOUT ACOUSTIC INTERVENTION AND $U_g = 3U_{mf}$.

Figure 6 shows the gas holdup as function of height for glass beads at two different superficial gas velocities. Figure 6 shows that at lower superficial gas velocity, the effects caused by the acoustic field are minimal – gas holdup is fairly uniform for both conditions. The main difference is that the acoustic condition has a lower bed expansion when U_g is fixed relative to U_{mf}.

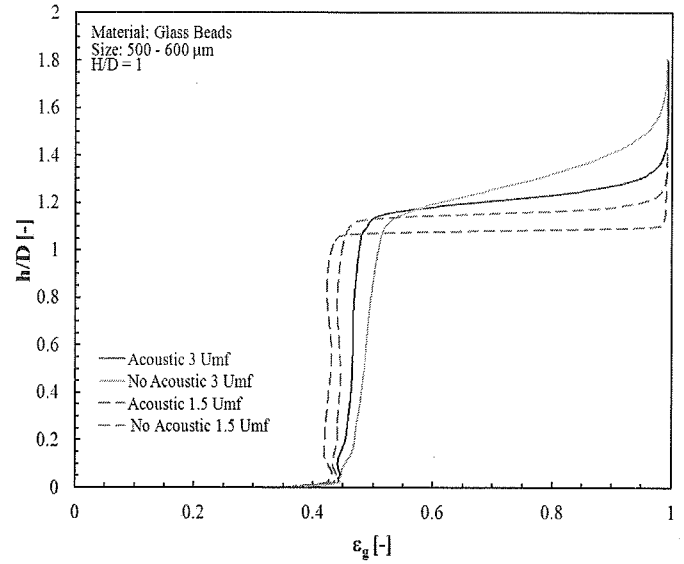

FIGURE 6: EFFECT OF SUPERFICIAL GAS VELOCITY ON HORIZONTAL AVERAGE GAS HOLDUP FOR DIFFERENT U_g AT H/D = 1.

Finally, local time-average gas holdup is plotted as a function of location along two mutually perpendicular lines that pass through the center of the bed for all the particle sizes tested at H/D = 1 and $U_g = 3U_{mf}$. Figure 7a) shows the local gas holdup data along the x-slice at an axial height h = 0.25D (2.5cm), while Figure 7b) shows the data along the y-slice. The local rise and fall in gas holdup is attributed to the presence of jets from the aeration plate.

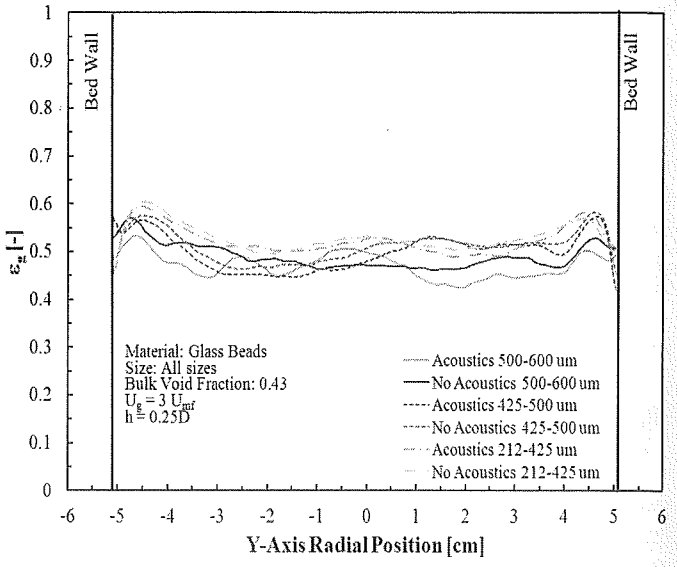

a)

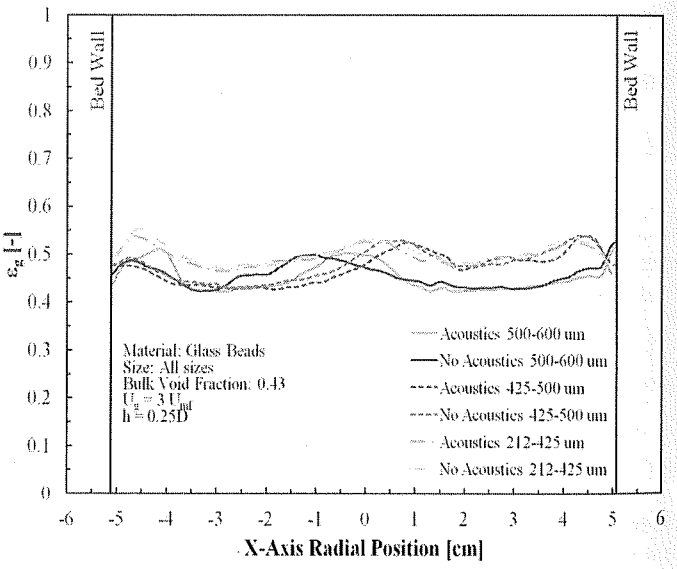

b)

FIGURE 7: a) X-SLICE LOCAL GAS HOLDUP, AND b) Y-SLICE LOCAL GAS HOLDUP, AS A FUNCTION OF LOCATION AT h = 0.25D FOR GLASS BEADS AT DIFFERENT SIZES.

It is observed in Figure 7a) and 7b) that the differences in the trends between acoustic and no acoustic curves for particles sizes of 212-425 µm and 425-500 µm are minimal, suggesting that acoustics does not produce effects in the hydrodynamic

behavior of the fluidized bed for these particle sizes. However, for 500-600 μm glass beads curves (green and blue solid lines on the figures) show that the acoustic curve present more rises and falls in the gas holdup (Figure 7a)) values due to local jets that have not yet merged with adjacent jets. In contrast, the no acoustic curve in the same radial position as the acoustic curve does not show these rises and falls in the gas holdup value, which may indicate that the local jet have lost their identity at that particular height into the bed. Further analysis of the local conditions will explore these differences more fully.

CONCLUSIONS

Local time-average gas holdup values obtained for fluidized beds filled with glass beads showed that the presence of an acoustic field produced a more uniform hydrodynamic structure compared to a fluidized bed without any acoustic intervention.

The acoustic field influenced the jetting phenomena present near to the aeration plate, the jets in the acoustic fluidized bed merged higher in the bed compared to the no acoustic condition, however acoustic fluidized beds have fewer amounts of active jets than the no acoustic fluidized bed conditions, which allowed to have a more homogeneous gas holdup region near the distributor plate.

Small particles in the size range 212-500 μm did not show any influence of acoustic intervention. Particles in the 500-600 μm range were influenced by acoustics and produced a more homogenous gas holdup for a fixed U_g relative to U_{mf}.

ACKNOWLEDGMENTS

The X-ray facility used in this work was developed with support from the National Science Foundation under Grant No. CTS-0216367 and Iowa State University. This work in this study was supported through Iowa State University.

REFERENCES

[1] Leu, L. P., Li, J. T. and Chen, C. M. (1997). "Fluidization of group B particles in an acoustic field." *Powder Technology,* **94**(1): 23-28.

[2] Guo, Q., Liu, H., Shen, W., Yan, X. and Jia, R. (2006). "Influence of sound wave characteristics on fluidization behaviors of ultrafine particles." *Chemical Engineering Journal.* **119**(1): 1-9.

[3] Kaliyaperumal, S., Barghi, S., Zhu, J., Briens, L. and Rohani, S. (2011). "Effects of acoustic vibration on nano and sub-micron powders fluidization." *Powder Technology,* **210**(2): 143-149.

[4] Levy, E. K., Shnitzer, I., Masaki, T. and Salmento J. (1997). "Effect of an acoustic field on bubbling in a gas fluidized bed." *Powder Technology,* **90**(1): 53-57.

[5] Herrera, C. A., Levy, E. K. and Ochs, J. (2002). "Characteristics of acoustic standing waves in fluidized beds." *AIChE Journal* **48**(3): 503-513.

[6] Guo, Q., Zhang, J. and Hao, J. (2011). "Flow characteristics in an acoustic bubbling fluidized bed at high temperature." *Chemical Engineering and Processing: Process Intensification,* **50**(3): 331-337.

[7] Si, C. and Guo, Q. (2008). "Fluidization characteristics of binary mixtures of biomass and sand quartz in an acoustic fluidized bed." *Industrial and Engineering Chemistry Research*, **47**(23): 9773-9782.

[8] Yates, J. G., Cheesman, D. J., Lettieri, P. and Newton, D. (2002). "X-Ray Analysis of Fluidized Beds and Other Multiphase Systems." *Kona,* **20**: 10.

[9] Heindel, T. J. (2011). "A Review of X-Ray Flow Visualization With Applications to Multiphase Flows." *Journal of Fluids Engineering-Transactions of the ASME,* **133**(7): 074001-074016.

[10] Escudero, D. (2010). "Bed height and material density effects on fluidized beds hydrodynamics". Department of Mechanical Engineering. Ames, IA, Iowa State University. **MSc. Thesis:** 109.

[11] Grassler, T. and Wirth, K. E. (2000). "X-ray computer tomography - potential and limitation for the measurement of local solids distribution in circulating fluidized beds." *Chemical Engineering Journal,* 77(1): 65-72.

[12] Escudero, D. and Heindel, T. J. (2011). "Bed height and material density effects on fluidized bed hydrodynamics." *Chemical Engineering Science,* **66**(16): 3648-3655.

[13] Escudero, D. and Heindel, T. J. (2012). Acoustic Field Effects on Minimum Fluidization Velocity in a 3D Fluidized Bed. 2012 ASME Fluids Engineering Summer Meeting. Puerto Rico, USA: 7. **FEDSM2012-72041**

[14] Heindel, T. J., Gray, J. N. and Jensen, T. C. (2008). "An X-ray system for visualizing fluid flows." *Flow Measurement and Instrumentation,* **19**(2): 67-78.

Proceedings of the

ASME Fluids Engineering Division Summer Meeting

– 2013 –

VOLUME 2

FORA

CAVITATION AND MULTIPHASE FLOW

FLUID MEASUREMENTS AND INSTRUMENTATION

MICROFLUIDICS SUMMER FORUM 2013

OPEN FORUM ON MULTIPHASE FLOWS: WORK IN PROGRESS

presented at

THE ASME 2013 FLUIDS ENGINEERING DIVISION SUMMER MEETING

JULY 7–11, 2013

INCLINE VILLAGE, NEVADA, USA

sponsored by

THE FLUIDS ENGINEERING DIVISION, ASME

A S M E

Two Park Avenue * New York, N.Y. 10016